



# Development of BNBSL: A $\beta$ - $\nu$ spectra library for spectrometry applications

G.W. Bailey\*, C. Dronne, D. Foster, M.R. Gilbert

United Kingdom Atomic Energy Authority, Culham Science Centre, Abingdon, Oxon, OX14 3DB, UK

## ARTICLE INFO

### Keywords:

Decay data  
Beta  
Antineutrino  
Activation  
Spectrometry  
Radioactivity

## ABSTRACT

While modern nuclear decay data can provide many details of a given nuclide's  $\beta$ -decay modes (branching ratios, decay heating etc.), knowledge of the emitted  $\beta$ -energy spectrum is often not included. This limitation hampers the use of decay data in some analysis, such as  $\beta$ -spectrometry of irradiated material, prediction of  $\beta$ -decay Bremsstrahlung or antineutrino,  $\bar{\nu}$ , detection. To address this deficiency, and for increased ease of  $\beta$ -spectrometry studies of complex samples, a library of  $\beta$ ,  $\nu$  and Bremsstrahlung-spectra, called BNBSL (Beta-Neutrino-Bremsstrahlung spectra library), has been produced. It has been found that the content compares favourably with experimental data and methodologies for its application to complex nuclear inventories have been developed. BNBSL contains spectra for over 1500 nuclides, which is hoped will benefit applied nuclear, radiation and materials science studies.

## 1. Introduction

Unlike  $\alpha$ - or  $\gamma$ -decay, the spectrum from  $\beta$ -decay is continuous, not discrete. This is because  $\beta$ -decay is a two particle emission process (a 3 body system with the daughter nucleus) producing either  $e^-$ ,  $\bar{\nu}_e$  or  $e^+$ ,  $\nu_e$ . The decay energy (minus daughter recoil) is shared between the two ejected particles. This energy is not similarly distributed for every decay event, thus giving continuous energy distributions for  $\beta - \nu$  emission rather than monoenergetic peaks.

Understanding the  $\beta$ -decay emission spectra has many applications. For example,  $\beta$ -emitting nuclei are used for internal radiotherapy and knowledge of the absorbed fraction (fraction of energy absorbed within a target volume) is essential for radionuclide internal dosimetry. As such complete knowledge of the range of emitted  $\beta$ -energies can be required for accurate radiation dose delivery (Ghorbani et al., 2019). Operators of nuclear fission power plants have interest in the  $\bar{\nu}$ -spectrum from a fission device as a remote monitoring and diagnostic tool (Huber, 2016).

$^3\text{H}$  accountancy will be essential for DT-fusion plants aiming for  $^3\text{H}$  self-sufficiency. Recent work (Shu et al., 2004; Matsuyama et al., 2005) has suggested that counting the Bremsstrahlung x-rays emitted during  $^3\text{H}$   $\beta^-$ -decay can be an effective in-situ method of determining  $^3\text{H}$  concentration. These works focused on tritiated water but previous work (Curtis, 1972) has shown that this approach can be applied to more complex systems such as hydrogen penetration into steel or  $^3\text{H}$  concentration contaminated pump oil.

All of these applications require some knowledge of  $\beta$ - $\bar{\nu}$ -spectra. However, while modern decay data libraries contain details of the

possible  $\beta$ -decay modes a nuclide can under go, knowledge of a given nuclide's complete  $\beta$ -(or  $\nu$ )-spectrum is often missing. This can make studies of  $\beta$ -spectra and related quantities, such as the associated  $\nu$ -spectra, cumbersome to perform for complex nuclear inventories. Meaning a complete radiological response of a given sample cannot be found using modern decay data alone.

So that these deficiencies can be addressed, a library of continuum  $\beta - \nu$  energy and Bremsstrahlung emission spectra for 1583 nuclides has been compiled. The library spectra have been derived from calculations using existing  $\beta$ -spectra codes and theory and  $\beta$ -decay transitions taken from the ENSDF (Evaluated Nuclear Structure Data File) database of the National Nuclear Data Center operated by Brookhaven National Laboratory (NNDC, 2019). This library is intended for applications to complex nuclear inventories, systems where many  $\beta$ -emitting nuclear species are present, such that relevant  $\beta - \nu$  or Bremsstrahlung spectra can be computed with relative ease.

### 1.1. Overview of relevant formalism

To aid discussion of  $\beta$ -decay properties this section gives an overview of formalism relevant to the library development.

#### 1.1.1. Transition spectrum and forbiddenness

A  $\beta$ -spectrum, in units of  $\beta$ 's per unit energy per disintegration, for a given decay is proportional to

$$N_{\beta}(E) \propto F(Z, E) C_L |\langle \Psi_f | \phi_{\beta} \phi_{\nu} | \hat{H} | \Psi_i \rangle|^2. \quad (1)$$

\* Corresponding author.

E-mail address: [greg.bailey@ukaea.uk](mailto:greg.bailey@ukaea.uk) (G.W. Bailey).

where  $N_\beta$  is the spectrum,  $E$  is the  $\beta$  kinetic energy and  $Z$  is the proton number of the daughter.  $F$  is the Fermi function which accounts for electromagnetic effects during the  $\beta$ -decay transition. The nuclear matrix element (NME,  $\langle \dots \rangle$  in Eq. (1)) describes the transition from the initial state in the parent nucleus,  $\Psi_i$ , to the final state in the daughter nucleus,  $\Psi_f$ .  $\phi_\beta$ ,  $\phi_\nu$  are the  $\beta$  and  $\nu$  wavefunctions respectively. The equivalent  $\nu$  spectrum,  $N_\nu$ , is the inverse of  $N_\beta$  due to the two decay products sharing total decay energy.

$C_L$  is the Shape factor, which details effects arising from the change in angular momentum transitioning from parent to daughter.  $L$  is the orbital angular momentum carried by the  $\beta - \nu$  pair which defines the *forbiddenness* of a given  $\beta$  transition. Early theories of  $\beta$ -decay assumed  $L$  was zero for all  $\beta$ -decay transitions, these transitions are called *allowed* transitions (if the total angular momentum,  $J$ , does not change the transition is called a *super-allowed* or a Fermi transition). It has since been observed that  $L > 0$  transitions do occur, these are referred to as *forbidden* transitions. The value of  $L$  determines a transitions order, for example  $L = 1$  is a 1st order *forbidden* transition. The  $\beta - \nu$  pair can have their spin angular momentum,  $S$  aligned ( $S = 1$ ) or unaligned ( $S = 0$ ). Transitions with  $S = 1$  are called *unique* transitions and their Shape factors can be analytically approximated. *Forbidden* transitions are typically less likely to occur than *allowed* transitions and so  $\beta$ -decaying nuclides which primarily undergo *forbidden* transitions typically have longer half-lives.

The impact of this *forbiddenness* on the spectrum manifests in the multiplicative factor  $C_L$  and in the NME. For allowed transitions  $C_0 = 1$  but a fully consistent form of  $C_L$  for all *forbidden* transitions has not been developed. While approximate forms for  $C_L$  have been derived, most Shape factors are determined experimentally (Mougeot, 2015b compiles a number of experimental measurements for example). The interaction Hamiltonian in the NME for *allowed* transitions can be defined

$$\begin{aligned} \hat{H} &= g_V \hat{1} \hat{\tau} \text{ Super Allowed,} \\ &= g_A \hat{\sigma} \hat{\tau} \text{ Allowed.} \end{aligned} \quad (2)$$

Here  $\hat{\tau}$  is the isospin transition matrix,  $\hat{\sigma}$  are the Pauli spin matrices and  $\hat{1}$  the unit operator.  $g_V$  and  $g_A$  are weak vector and axial vector coupling constants. The interaction Hamiltonian, and therefore the matrix elements, for *forbidden* transitions are non-trivial and still require development. Determining the correct form for the NME can be a source of significant uncertainty in  $\beta$ -decay theory. For example,  $N_\beta$  have been shown to be sensitive to the value of  $g_A$  (Leder et al., 2022; Bodenstern-Dresler et al., 2020).

### 1.1.2. Mean spectrum energy and total spectrum

Once a  $\beta/\nu$  spectrum has been calculated its mean energy,  $\bar{E}$  can be found via:

$$\bar{E} = \frac{\int_0^\infty E N_\beta(E) dE}{\int_0^\infty N_\beta(E) dE}. \quad (3)$$

It is not uncommon for a nucleus to be able to undergo many different  $\beta$ -decay transitions, from the same initial state to differing final states, with differing transition rates. As such the energy spectrum observed, the total  $\beta$ -spectrum  $N_{total}$ , will be a sum, weighted by the transition rates, of the possible transition spectra,

$$N_{total}(E) = \sum_j^{t_n} N_j(E) p_j, \quad (4)$$

where  $p_j$  is the transition probability defined such that their set sums to unity and  $t_n$  is the number of transitions a nuclide can undergo.

It should be noted that the total  $\nu$ -spectrum is only guaranteed to be the energetic inverse of the total  $\beta$ -spectrum in cases where only a single transition occurs. For nuclides which can undergo several  $\beta$ -transitions the total  $\nu$ -spectrum must be found from the sum of

transition  $\nu$ -spectra using the relationship in Eq. (4). Therefore, such a total  $\nu$ -spectrum will need to be treated separately from the total  $\beta$ -spectrum. For applications to systems containing many  $\beta$ -emitting nuclides,  $N_{total}$  ( $\beta$  and  $\nu$ ) will have to be known for each nuclide.

Due to  $N_{total}(E)$  being a composite spectrum of different transitions (with different changes in angular momentum) defining its absolute *forbiddenness* and *uniqueness* is not possible. Metrics can be defined using transition probabilities,  $p$ , to assess the contribution from *forbidden* transitions for transition order,  $L$ ,

$$\begin{aligned} f_L^n &= \sum_j P_{L,j}^{non-unique}, \\ f_L^u &= \sum_j P_{L,j}^{unique}, \\ f_L^a &= \sum_j P_{L,j}^{allowed}. \end{aligned} \quad (5)$$

Here  $p^{non-unique}$ ,  $p^{unique}$ ,  $p^{allowed}$  are the transition probabilities for *unique*, *non-unique* and *allowed* transitions for a given  $L$ .  $f_L^n$ ,  $f_L^u$ ,  $f_L^a$  give a measure of contribution to the total spectrum arising from different types of transitions of order  $L$ . Due to the complete set of  $p$  summing to unity,

$$\sum_L f_L^n + f_L^u + f_L^a = 1 \quad (6)$$

For example if  $f_2^u = 0.8$  it would inform that 80% of the transitions which contribute to the total spectrum were 2nd order *unique* transitions.

### 1.1.3. Q-value vs. end-point energy

The Q-value for  $\beta$ -decay can be defined as

$$Q = (m_p - m_D - m_e - m_\nu)c^2. \quad (7)$$

In Eq. (7)  $m_p$  and  $m_D$  are the masses of the parent and daughter nuclei.  $m_e$  is the electron/positron mass and  $m_\nu$  (anti-)neutrino mass.  $c$  is the speed of light. If a nucleus  $\beta$ -decays to the ground state of the daughter the Q-value gives the highest kinetic energy an emitted  $\beta$  could have and will define the end point of a  $\beta$ -spectrum. Many  $\beta$ -transitions result in final states with non-zero excitation energy  $E_{exc}$ , for these transitions the highest kinetic energy which can be achieved will be modified by the excitation energy of the final state. This gives the definition of a  $\beta$ -spectrum's end-point energy,  $E_{end}$ , as

$$E_{end} = Q - E_{exc}. \quad (8)$$

$E_{end}$  for a total spectrum will equal to the greatest  $E_{end}$  for the transition spectra included in its construction, if these include a transition to the ground state it will be equivalent to the Q-value.

### 1.1.4. Internal bremsstrahlung

As a  $\beta$ -particle leaves its parent nucleus and traverses the atom, like all charges moving through an electric field, it will emit Bremsstrahlung photons. This effect is referred to as *internal* Bremsstrahlung, as it occurs within the atom. Once the  $\beta$ s have escaped the atom they will interact with the surrounding medium and continue to emit Bremsstrahlung photons. This *external* Bremsstrahlung requires knowledge of the surrounding material and geometry, which is beyond the scope of the present work. Typically these photons are peaked low energy, but their range can be extended if the emitted  $\beta$  is of high enough energy. The contribution of Bremsstrahlung photons to expected photon dose rates can be an important consideration in analysis of nuclear devices.

Expressions for *internal* Bremsstrahlung emission were found by Knipp and Uhlenbeck (1936) and independently Bloch (1936), hence this is referred to as KUB theory. Despite this formalism assuming only allowed transitions, it has been shown to be valid for several forbidden decays (Chang and Falkoff, 1949; Cengiz and Almaz, 2004), but a full complete theory has yet to be developed.

The probability,  $S$ , of a Bremsstrahlung photon being emitted with energy  $E_\gamma$  per  $\beta$ -decay (as defined by Knipp and Uhlenbeck, 1936; Boehm and Wu, 1954) is given by

$$S(E_\gamma) = \int_{1+E_\gamma}^{E_{max}} N_\beta(E_\beta) \frac{\alpha p'}{\pi p E_\gamma} \left[ \frac{E_\beta^2 + (E_\beta - E_\gamma)^2}{E_\beta p'} \times \ln(E_\beta - E_\gamma + p') - 2 \right] dE_\beta. \quad (9)$$

where  $E_\gamma$  and  $E_\beta$  are the photon and  $\beta$  energies respectively,  $p$  and  $p'$  are the  $\beta$  momenta before and after the emission of a photon with energy  $E_\gamma$ .  $\alpha$  is the fine structure constant.  $E_{max}$  is the maximum possible  $E_\beta$  for a given transition. The lower limit is due to the condition that  $E_\beta \geq E_\gamma$  to produce a photon with energy  $E_\gamma$ .

The number of photons emitted within a given energy interval is found by integrating  $S$  over the interval,

$$I_k = \int_{E_i}^{E_j} S(E_\gamma) dE_\gamma. \quad (10)$$

where  $k = E_j - E_i$  defines the energy interval of interest. The photon rate (per unit time) can be found via the product of  $I_k$  with a given nuclide's activity, which can be used to calculate a photon emission power for photon dose rate predictions.

## 2. Available $\beta$ -spectra data

Before development of a new data set, a review of the currently available  $\beta$ -continuum spectra was performed. This includes evaluated decay data libraries and other data sets developed for specific applications.

### 2.1. Evaluated decay data libraries

It may seem reasonable to assume that a  $\beta$ -spectrum library could be constructed from existing evaluated decay data. However, the ENDF-6 (Evaluated Nuclear Data File) format used by decay data libraries has some limitations which hinder a complete description of  $\beta$ -decay being included. The ENDF-6 format (Group, 2018) allows decay spectra to be stored as either discrete line data, full continuum data or both. In either case the spectrum's mean energy and, in the case of  $\beta$ -decays, whether the decay is Fermi (*super-allowed*) or Gamow-Teller (*allowed/first forbidden*) can be included. Unfortunately only a single continuum spectra can be included per decay mode. As such, knowledge of the different  $\beta$ -transitions spectra or separate information on  $\nu$ -spectra cannot be included.

$\beta$ -decays in ENDF-6 format are identified as either  $\beta^-$  or  $\beta^+$  + electron – capture (*e.c.*). Electron capture is a process where-by an atomic electron is captured by a proton, which transitions to a neutron releasing a  $\nu_e$ . Afterwards, either an atomic electron will de-excite to fill the vacated level, emitting a photon, or the atom will eject an outer electron, the Auger effect. This process competes with  $\beta^+$ -decay, as they produce the same daughter. Electron capture and  $\beta^+$ -decay being non-separable in ENDF-6 data is troublesome, making it difficult to study  $\beta^+$ -decay fully with such data libraries.

Due to these issues data originating in ENDF-6 format will likely be incomplete and therefore not sufficient to construct a library. Table 1 shows the details of  $\beta$ -spectra given in 4 modern decay data libraries: decay2020, a composite decay library produced by UKAEA (decay2020, 2021), JEFF3.3 (Plompen et al., 2020), ENDF/BVIII (Brown et al., 2018) and JENDL5 (Iwamoto et al., 2020). These show that many radionuclides with a  $\beta$ -decay mode do not include any spectral information and those that do often only contain discrete line data. The intended physical interpretation of a discrete  $\beta$ -spectra is assumed to represent the daughter energy levels and the relative intensity ( $p_j$  in Eq. (4)) of each possible  $\beta$ -decay transitions a nucleus is expected to

**Table 1**

The number of nuclides with available  $\beta^-$  and  $\beta^+ / e.c$  spectra in the decay data libraries decay2020, JEFF3.3 ENDF/BVIII and JENDL5.

Library	$\beta^-$ -decay mode			
	Can $\beta^-$ decay	Has $\beta^-$ spectra	Continuum spectra	Discrete spectra
decay2020	1526	929	160	774
JEFF3.3	1374	705	33	672
ENDF/BVIII	1359	1014	276	738
JENDL5	1509	1369	446	923
Library	$\beta^+ / e.c.$ -decay mode			
	Can $\beta^+$ decay	Has $\beta^+$ spectra	Continuum spectra	Discrete spectra
decay2020	1669	774	0	774
JEFF3.3	1657	579	0	579
ENDF/BVIII	1564	685	0	685
JENDL5	1422	888	0	888

undergo. While this data may be useful to calculate a continuum spectrum for a given nuclide, such a computational burden is cumbersome and may not be within the capabilities of some analysis or processing codes/techniques.

All of the libraries studied do include some continuum  $\beta^-$ -spectra, but only a minority of  $\beta$ -emitting nuclides are covered. The available continuum spectra would not provide adequate coverage of the nuclear landscape to be used reliably in most applications. Interestingly, no library includes any continuum spectra for  $\beta^+$  emissions. This is likely a consequence of the ENDF-6 format mixing  $\beta^+$  and *e.c* decays, making including a continuum spectrum problematic. Table 1 demonstrates that not only are there limitations to the ENDF-6 format, but libraries making use of the format do not contain complete description of  $\beta$ -decay.

For most libraries, the nuclides which have evaluated continuum spectra are typically part of fission chains. This is likely a consequence of the evaluations used in these libraries targeting nuclear fission monitoring applications discussed in Section 1. As noted in Section 1.1, if a nuclide can undergo several different  $\beta$ -decay transitions taking the inverse of the supplied total  $\beta$ -spectrum may not provide an accurate representation of the corresponding  $\nu$ -spectrum. This implies that, despite the increased effort to provide continuum spectra, those provided may not be fully appropriate for some applications.

### 2.2. RADAR database

$\beta$ -spectra are of importance to health physics and a number of relevant spectra have been calculated. These have been stored in an existing database called RADAR, the RADiation Dose Assessment Resource (RADAR decay data, 2019). These spectra were calculated with the code EDISTR04, an updated version of EDISTR (Dillman, 1980) from data in ENSDF format, from the NNDC (NNDC, 2019). The technical basis for these continuum spectra for use in health physics has been published (Eckerman et al., 1994; Stabin and da Luz, 2002). Spectra found with EDISTR have been used as part of decay data development by the International Commission on Radiological Protection (ICRP) (ICRP, 2008) targeting dosimetric applications. This data set does not include enough nuclides to be reliably used for general activation applications, however this data can be used to validate calculated spectra.

## 3. Available $\beta$ -spectrum calculators

There has been some effort by the theoretical physics community to calculate  $\beta$ -spectra with high degrees of accuracy. Codes have recently been produced which are capable of computing complete  $\beta - \nu$  spectra. Two of these have been investigated as possible candidates to construct

the desired  $\beta - \nu$  spectra library. All methods discussed assume a zero-mass  $\nu$ .

*BetaShape* (Mougeot, 2017) is a code developed by Mougeot. It is the result of several studies of phenomenological  $\beta$ -decay shape factors (Mougeot, 2015c,a,d). *BetaShape*, as its name suggests, has put significant effort in to accounting for shape factors and as such is able to evaluate  $\beta$  spectra for some forbidden transitions. *BetaShape* includes over a hundred phenomenological shape factors for different nuclides. If one of these shape factors is not found, *BetaShape* can use the approximation,

$$C_L(p, q) = (2L - 1)! \sum_{k=1}^L \lambda_k \frac{p^{2(k-1)} q^{2(L-k)}}{(2k-1)! [2(L-k)+1]!}, \quad (11)$$

where  $p$  and  $q$  are the  $\beta$  and  $\nu$  momenta, respectfully. This approximation is only valid for *unique* transitions but it has been shown that  $C_L$  for 1st order *forbidden* transitions can deviate from this approximation if a more complete form of the NME (see Eq. (1)) is used (Hayen et al., 2019a,b). Due to these factors *BetaShape* cannot be said to fully account for forbidden transitions. The code was partially developed to aid nuclear data analysis and as such can read ENSDF data directly. *BetaShape* also includes uncertainties as part of its output; these are determined from uncertainties within the relevant ENSDF file and propagated through the calculations.

Another code, *Beta Spectrum Generator* (BSG) is an open-source C++ code developed by Hayen and Severijns (2019) which can calculate continuum  $\beta$  and  $\nu$  spectra. This was written to supply the particle physics community with accurate  $\beta$ -spectra. These are required as part of the search for Beyond Standard Model physics such as neutrino inverted hierarchy and the possibility that neutrinos are Majorana fermions (their matter and antimatter equivalents are identical). BSG cannot account for forbidden transitions but can include a host of minor correction factors which arise from nuclear and atomic effects.

Comparison between spectra found from *BetaShape* and BSG for allowed transitions showed that they produce quantitatively the same spectra, but differ for forbidden transitions as expected. Example spectra from BSG and *BetaShape* for  $^{14}\text{C}$ ,  $^{39}\text{Ar}$  and  $^{98}\text{Tc}$  which undergo a single transition, are shown in Fig. 1 alongside data taken from the RADAR database. Here the spectra agree for the *allowed* transition of  $^{14}\text{C}$ , but deviate for the *forbidden* transitions of  $^{39}\text{Ar}$  and  $^{98}\text{Tc}$ . *BetaShape* and RADAR agree for the *unique* transition of  $^{39}\text{Ar}$ , but show deviation for the *non-unique*  $^{98}\text{Tc}$  transition. This is an example of the ambiguities associated with spectra from *non-unique* transitions.

## 4. The $\beta - \nu$ spectra library

### 4.1. Library construction and content

Given its ability to calculate spectra beyond allowed transitions, *BetaShape* was chosen to construct BNBSL using nuclear structure data taken from NNDC ENSDF (NNDC, 2019). The calculations included the screening (Bührling, 1984) and radiative (Sirlin, 1967, 2011) corrections available as options with *BetaShape*. As the library is intended for use with complex nuclear inventories, the total spectra will need to be summed within these applications. To facilitate this all spectra are stored on a 1 keV grid spacing, from 0 keV up to their total spectrum's end-point energy. All spectra within the library are normalised to unit area under the spectrum curve and the mean energies for each spectrum are included.

The ability to rapidly assess the expected internal Bremsstrahlung from a single nuclide or set of nuclides is not viable from current decay data. To address this, the emission probabilities,  $S$  (Eq. (9)), have been found for each nuclide included. From this the  $\gamma$ -intensity,  $I_\gamma$  in Eq. (10), can be found for which-ever  $\gamma$ -binning structure a user desires.

The library contains total  $\beta - \nu$  spectra and Bremsstrahlung probabilities for 1583 nuclides. A brief summary of the library content is

**Table 2**

A summary of the  $\beta - \nu$  spectra library. Note that some nuclides are both  $\beta^-$  and  $\beta^+$  emitters. Here  $Z$  is a nuclides atomic number and  $t_{1/2}$  its half-life. The library has entries for some primordial nuclides, hence a large maximum  $t_{1/2}$ .

	Library content
Total nuclides	1583
$\beta^-$ -emitters	909
$\beta^+$ -emitters	694
$Z_{min}$	1
$Z_{max}$	101
min $t_{1/2}$	$0.0022 \pm 0.0001$ s
max $t_{1/2}$	$8.3 \times 10^{24} \pm 2 \times 10^{16}$ s

given in Table 2 and its coverage of the nuclear landscape is visualised in Fig. 2.

The  $\beta^-$ ,  $\gamma$  and  $\beta^-$ -induced Bremsstrahlung spectrum for  $^{131}\text{I}$ , Fig. 3, and  $^{99}\text{Mo}$ , Fig. 4, are shown as examples. Studying the lower panel of Fig. 3 reveals that the  $\beta^-$ -spectrum for this nuclide is dominated primarily by two transitions; 364 keV allowed and 163keV 1st order forbidden, but all transitions were included in the total spectrum's calculation. Here the energies stated are the excitation energies in the daughter nucleus. The good agreement seen between the total spectrum and the data taken from RADAR. This is likely a consequence of the nuclear structure inputs sharing common origin and the contribution from *non-unique forbidden* transitions being small for  $^{131}\text{I}$ . However, the equivalent spectra for  $^{99}\text{Mo}$  (lower panel of Fig. 4) shows that good agreement can be achieved for nuclides with total spectra dominated by *non-unique forbidden* transitions.

The photon spectra presented in the upper panels of Figs. 3 and 4 show the low energy peak of the Bremsstrahlung photons taken from the Library (filled curve). It can also be seen that the Bremsstrahlung photons can extend to higher energies with comparable intensities to some observed  $\gamma$ -lines and could have a noticeable contribution to photon dose rate predictions.

### 4.2. Validation

In order to assess the continuum spectra comparisons to existing data have been performed. The data used here is taken from (i) Rudstam et al. (1990) experiments which measured the  $\beta$  and  $\gamma$  spectrum from a number of fission relevant nuclides (ii) Algora et al. (2021) and Valencia et al. (2017) total absorption spectroscopy (TAGS) measurements and (iii) the RADAR database.

Some comparisons to Rudstam et al. (1990), alongside value of reduced chi-square,  $\chi_v^2$ , and the R-squared coefficient of determination,  $R^2$ , are shown in Fig. 5. Reduced chi-square and the R-squared coefficient of determination are defined as

$$\chi_v^2 = \frac{1}{\nu} \sum_i \frac{(M_i - N_i)^2}{\sigma_i^2} \quad (12a)$$

$$R^2 = 1 - \frac{\sum_i (M_i - N_i)^2}{\sum_j (M_j - \bar{M})^2}. \quad (12b)$$

In Eqs. (12a) and (12b)  $M$  is the measured experimental spectrum,  $\sigma$  its associated uncertainty and  $\bar{M}$  the mean of the experimental values.  $\nu$  the number of data points and  $N$  the library spectrum compared to.

A  $\chi_v^2$  value close to 1 indicates that the difference between the experiment and the model is of similar magnitude to the uncertainty, hence the model reproduces the data. If the uncertainties are large  $\chi_v^2$  can be far from 1 even if the model predicts the data points well.  $R^2$  informs how well a model prediction can account for the variance in the data.  $R^2$  should be between 0 and 1, with a value of exactly 1 meaning a model fully reproduces the data points.

In this analysis  $R^2$  gives a measure of how well the library spectra can reproduce the experimental data points while  $\chi_v^2$  informs as to how well the prediction agrees within uncertainty. Generally  $\chi_v^2$  is more

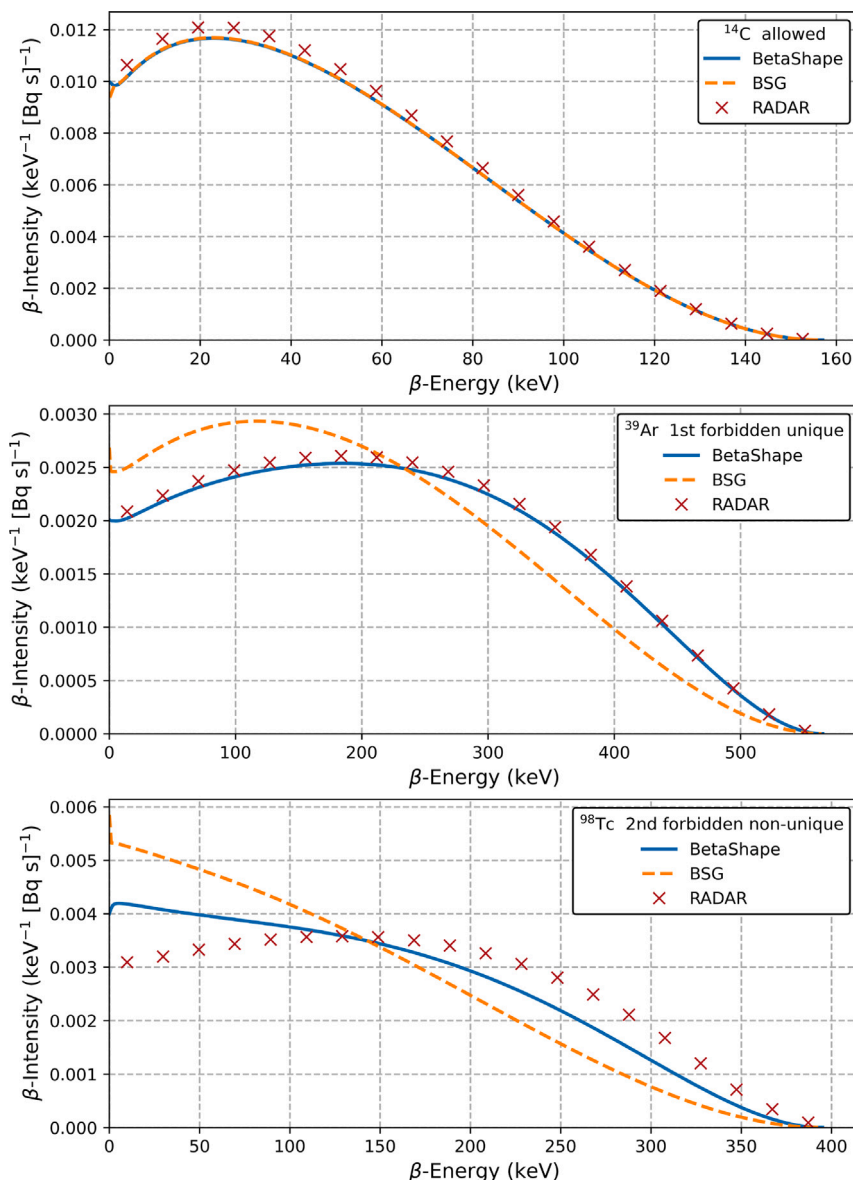


Fig. 1.  $\beta$  spectra from  $^{14}\text{C}$  (upper panel),  $^{39}\text{Ar}$  (middle panel) and  $^{98}\text{Tc}$  (lower panel) calculated with *BetaShape* and *BSG*, compared to data from *RADAR*.  $\beta$ -energy is the kinetic energy of the  $\beta$ . Each nuclide undergoes a single  $\beta$ -transition so these are equivalent to the total spectrum.

favourable when comparing to experiment but  $R^2$  give a useful measure when uncertainties are large or unavailable.

For all of the nuclides shown in Fig. 5 the *BetaShape* spectra show good qualitative agreement with the experimental data, however  $^{90m}\text{Rb}$  and  $^{95}\text{Sr}$  show poorer low energy agreement. For experimental data which have larger associated errors, such as those shown for  $^{81}\text{Ge}$ ,  $^{90m}\text{Rb}$  and  $^{98}\text{Sr}$ , the calculated spectra are able to describe the shape and magnitudes of the data well, even if the fit is statistically poor ( $\chi^2_\nu$  and/or  $R^2$  far from 1). The experiments in Rudstam et al. (1990) used different detectors for the low ( $\leq 1$  MeV) and high energy components of the measured spectrum. This may account for some of the variance in the data at such energies.

The largest of the *forbiddenness* metrics (defined in Eq. (5)) is also shown for each nuclide in Fig. 5 as well as the number of transitions contributing to the total spectrum. Studying the *forbiddenness* metric does not reveal a strong correlation between significant contribution from *forbidden* transitions and poor fits. All of the decays presented in Fig. 5 which have large contributions from *non-unique forbidden* are first order,  $L = 1$ . In Mougeot (2015c,a) it is shown that some *non-unique forbidden* transition can be reproduced by *BetaShape*'s approximations.

It should also be noted that these are total spectra, with between 9 and 58 transitions contributing, so the exact impact of the treatment of *forbiddenness* is difficult to determine.

A complete comparison was made between the gathered data and those calculated with *BetaShape* via  $R^2$  analysis (as defined in Eq. (12b)), this was chosen as the data taken from the *RADAR* database does not have associated errors so  $\chi^2_\nu$  cannot be used. A summary of the results are shown in Fig. 6. It is clear that most spectra show good agreement, with the vast majority of spectra having  $R^2 \geq 0.9$ . This implies that we can have some confidence in the *BetaShape*-derived library, as many  $\beta$ -spectra appear accurately represented. The *forbiddenness* metrics (Eq. (5)) were calculated for each nuclide, and separate tallies found for those with the largest contribution from *forbidden* and *forbidden non-unique* transitions. Fig. 6 shows that there is no strong correlation between *forbiddenness* or *uniqueness* and poor agreement, the tallies show the same trend as that for the complete set of nuclides. This is further evidence that the *BetaShape* spectra are able to describe some *forbidden non-unique* transitions. It should be noted that only 14 nuclides have total spectra with dominant contributions from transitions of order 2 or greater. Therefore *BetaShape*'s ability to

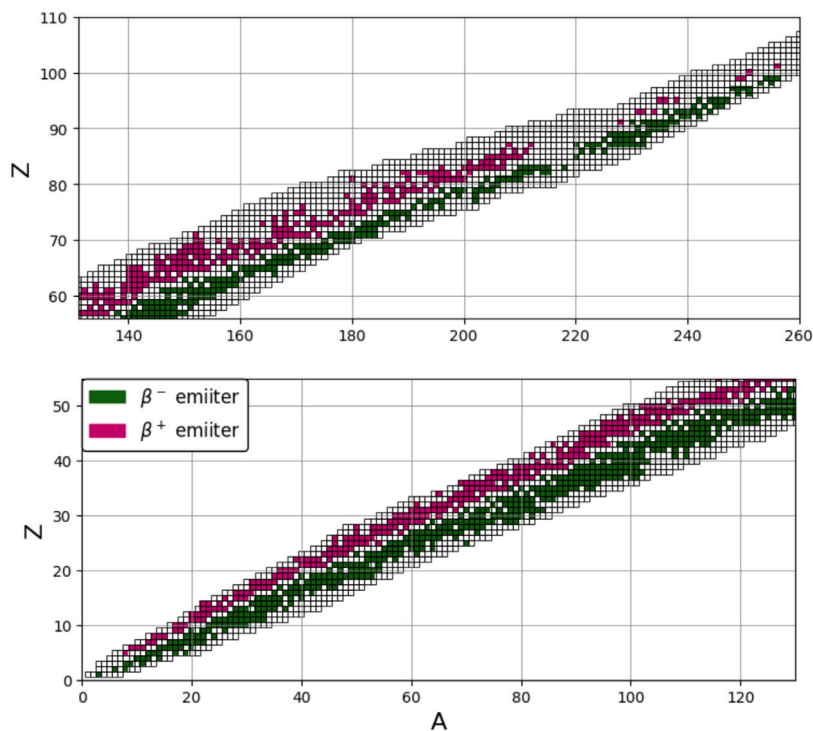


Fig. 2. A plot of the nuclear chart with nuclides included in the library shaded. The library content covers a large range of the nuclear chart.

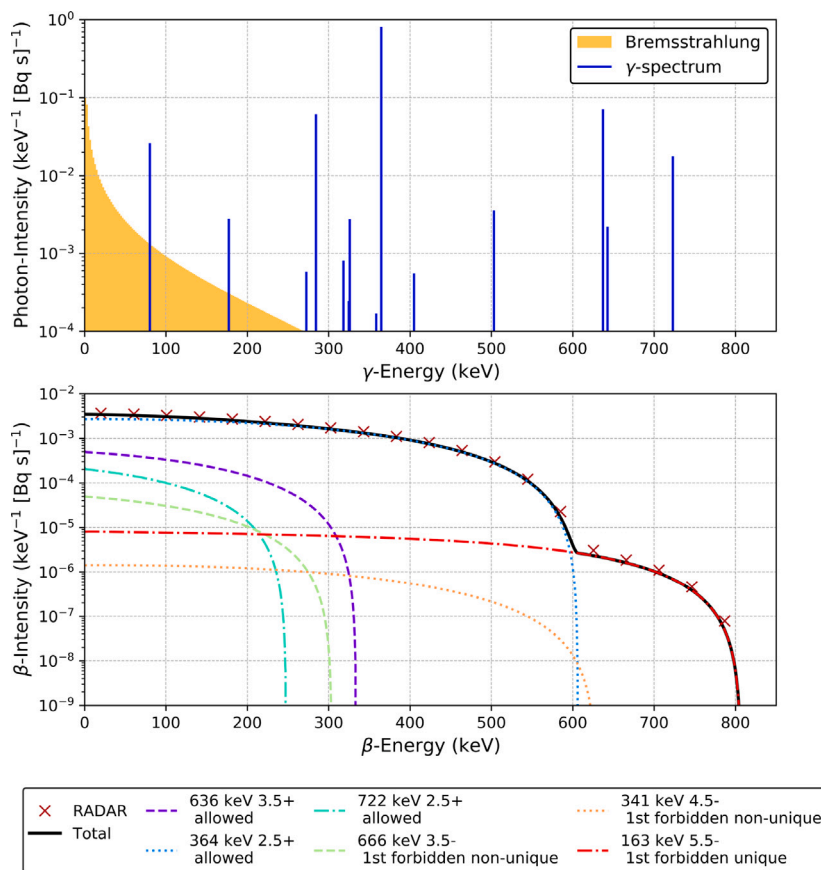


Fig. 3. An example of BNBSL spectra for  $^{131}\text{I}$ . The upper panel shows the  $\gamma$  (taken from decay2020) and  $\beta^-$ -induced Bremsstrahlung spectrum (2 keV intervals), the lower panel the  $\beta^-$  spectrum.  $\beta$ -energy is the kinetic energy of the  $\beta$ . The lower panel shows the total spectra alongside the spectra from  $^{131}\text{I}$ 's individual  $\beta^-$ -decay transitions. Also include are data from the RADAR database as points. The values given in the legend are the excitation energy and spin-parity of the final state.

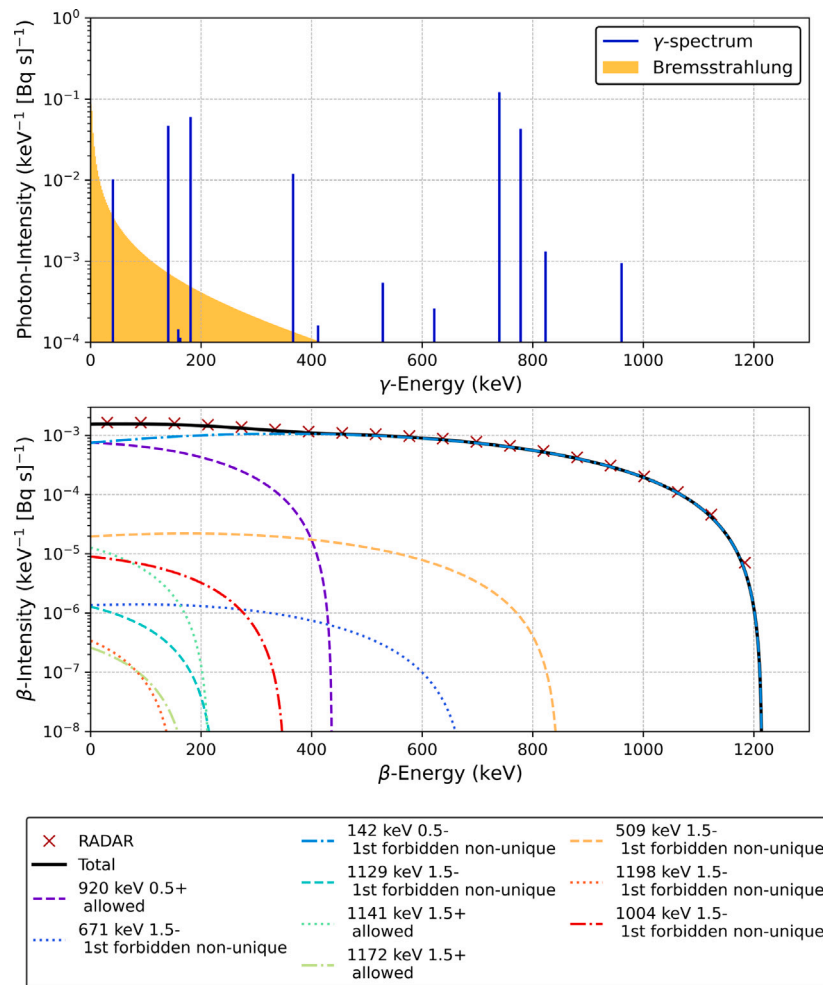


Fig. 4. An example of BNBSL spectra for  $^{99}\text{Mo}$ . The upper panel shows the  $\gamma$  (taken from decay2020) and  $\beta^-$ -induced Bremsstrahlung spectrum (2 keV intervals), the lower panel the  $\beta^-$  spectrum.  $\beta$ -energy is the kinetic energy of the  $\beta$ . The lower panel shows the total spectra alongside the spectra from  $^{99}\text{Mo}$ 's individual  $\beta^-$ -decay transitions. Also include are data from the RADAR database as points. The values given in the legend are the excitation energy and spin-parity of the final state.

describe higher order *forbidden non-unique* transitions is not well probed in this study. These results suggest that improvements can be made but whether improved modelling or more complete input data is required will be nuclide specific.

#### 4.2.1. Mean energy comparison

The experiments described in Rudstam et al. (1990) also recorded the mean  $\beta$ -energies for the nuclides studied. Each of these has been compared to those from the *BetaShape* derived library (using Eq. (3)) and those present in the Nuclear Data libraries investigated in Section 2 (see Table 1). This is presented as a ratio of the calculated values over the experimental values (C/E) for 99 nuclides in Fig. 7.

The C/E results show a significant amount of agreement between the *BetaShape*-derived library and the values taken from evaluated Nuclear Data with the experimental results. However, there are several nuclides where this is not true and further study did not reveal a correlation with dominant contribution from *forbidden* transitions. For several nuclides with poor agreement, such as  $^{80}\text{Ga}$  and  $^{84}\text{As}$ , the  $\beta$ -library and Nuclear Data are clustered, suggesting similar source data used to determine the mean energies. This can also be observed for  $^{130m}\text{Sn}$ , which shows the largest deviations from the experimental values. It can be concluded from these results that the mean spectrum energies taken from the  $\beta$ -library, are of a similar quality to those from evaluated decay data libraries. However, Fig. 7 also highlights issues around some nuclides  $\beta$ -decay data, suggesting further experiments are required and/or more rigorous consideration of the nuclear matrix elements and shape factors (see Eq. (1)).

## 5. Methodology of application of the $\beta - \nu$ spectra library

### 5.1. Storage and formatting

Given the unique requirements of the data, the traditional ENDF-6 library format is inappropriate. The format would not allow for the storage of multiple continuum spectra per decay mode. It was decided to store the data in JSON format with a bespoke schema, details of which is provided alongside the data. JSON format was chosen for its readability and compatibility with modern computing. The data library, a manual and methods are available on the FISPACT-II Nuclear Data download page (UKAEA, 2023).

### 5.2. Methods for inventory spectra

The  $\beta$  or  $\nu$  spectrum for a complete inventory,  $\mathcal{N}$ , of nuclides can be found from the weighted sum of individual nuclide spectra,  $N_i$ . The sum weighting is found from a nuclide's activity (nuclear disintegration's per second),  $A_i$ , in a given inventory and its total  $\beta$ -decay branching ratio,  $b_i$ , such that

$$\mathcal{N}(E) = \sum_i^m b_i A_i N_i(E). \quad (13)$$

Here  $E$  is the  $\beta$  or  $\nu$  energy and  $m$  is the number of nuclides present in the inventory. Weighting the nuclide's activity by  $b$  allows the correct amount of  $\beta$ -decays to be accounted for, as only  $\beta$  emitting

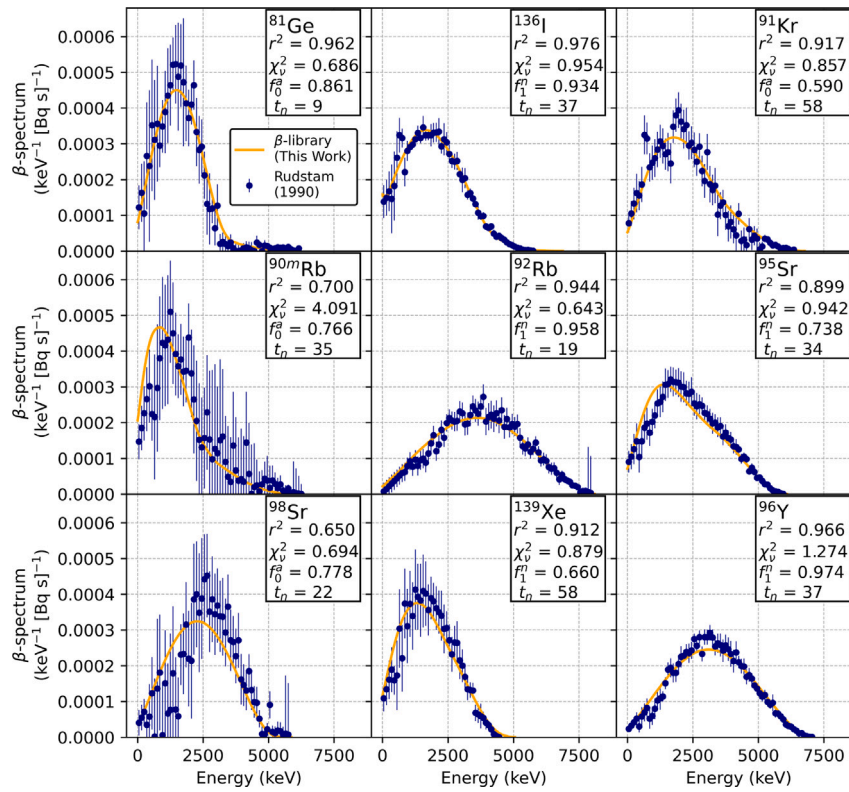


Fig. 5. Total  $\beta^-$  spectra for a number of nuclides with available experimental data taken from Rudstam et al. (1990). Energy is the kinetic energy of the  $\beta$ . Calculated spectra using BetaShape (solid lines).  $\chi^2_{\nu}$  and  $R^2$  values are given for each spectrum. The largest forbiddenness metric as defined in Eq. (5) and the number of transitions,  $t_n$  are also shown.

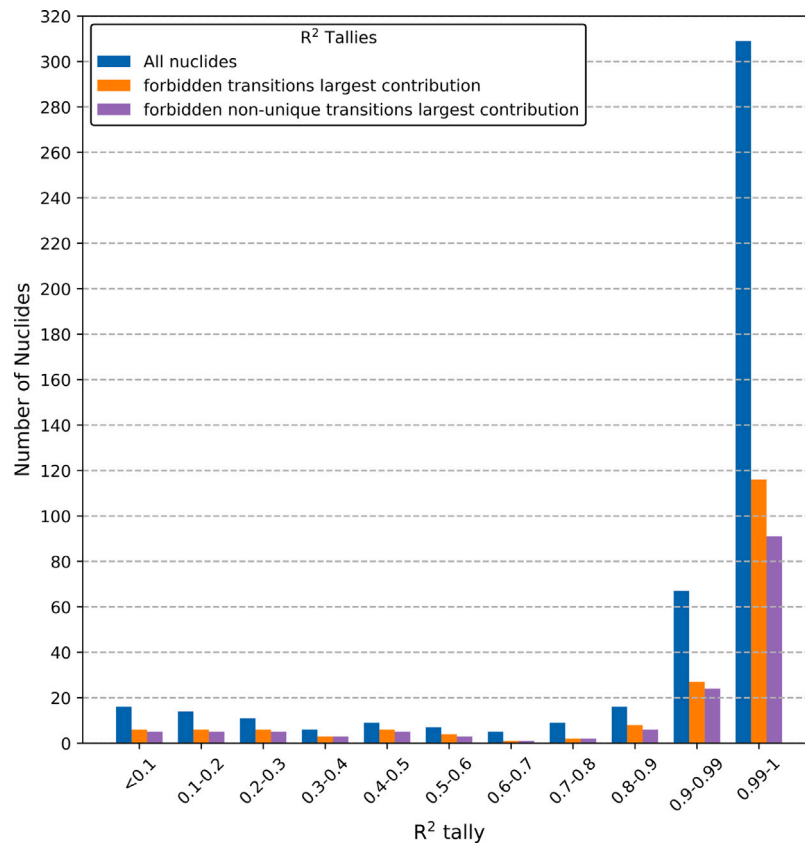


Fig. 6. Tallies of  $R^2$  values comparing the BetaShape-derived library and available continuum spectra. All calculated  $R^2$  were positive. Tallies are also included for nuclides which have total spectra with the largest contribution from forbidden and non-unique transitions (as defined by Eq. (5)).

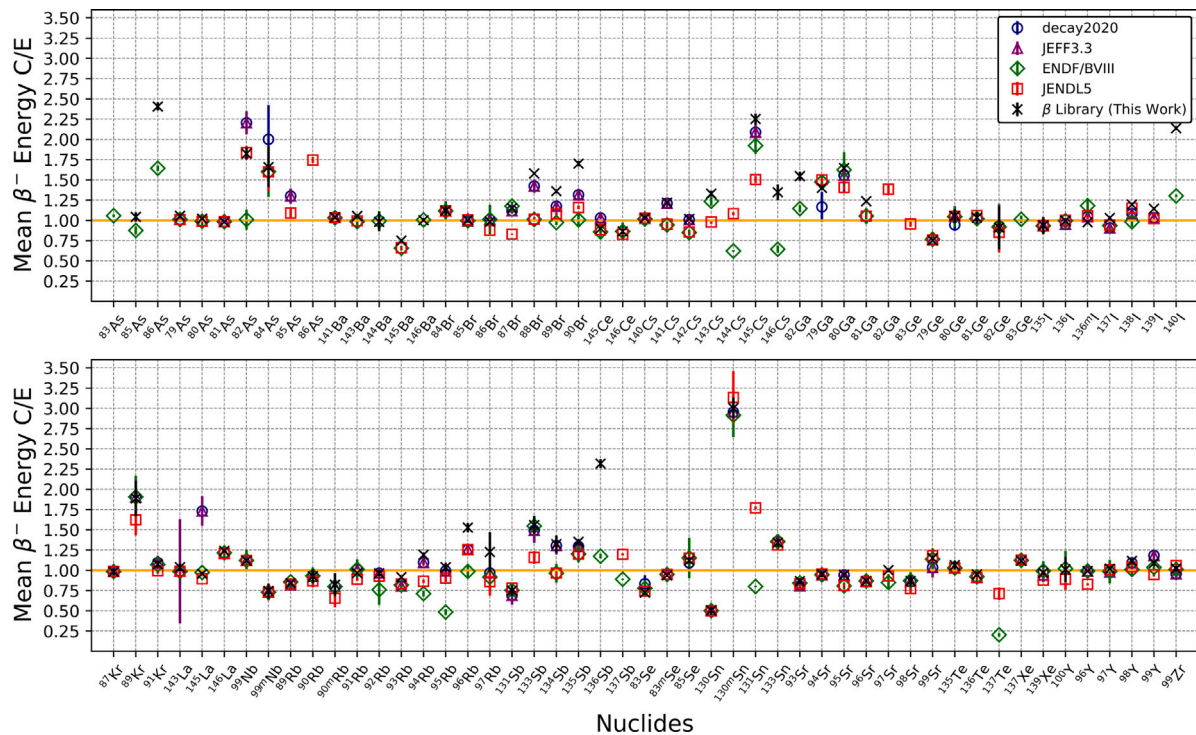


Fig. 7. Calculated over experimental (C/E) values for the mean  $\beta^-$ -energies for nuclides whose spectra were measured in Rudstam et al. (1990). The uncertainties in C/E given were propagated from those in the experiment and the calculated values.

disintegrations will be included. Eq. (13) gives an inventories  $\beta$  or  $\nu$  spectrum in emitted particles per unit energy per second. The internal Bremsstrahlung contribution to a complex inventory's  $\gamma$ -spectrum can be found by summing the intensity spectra,  $I_\gamma$  (Eq. (10)), for each nuclide. As with the  $\beta$ -spectrum this sum is weighted by a given nuclide's activity,  $A_i$ , and  $\beta$ -decay branching ratio,  $b_i$ .

$$I = \sum_i^m A_i b_i I_i, \quad (14)$$

this gives the spectrum in  $\gamma$ 's per second per energy interval. Like  $I_\gamma$ ,  $I$  can be multiplied by the energy interval to find Bremsstrahlung photon emission power for photon dose rate calculations.

### 5.3. Example: Tungsten as fusion reactor first wall

During fusion reactor operation high energy (14.1 MeV) neutrons will bombard the reactor structure. Many current fusion reactor concepts are considering Tungsten armour as part of the so called *first wall* material, that which is closest to the fusion neutron source. As such, understanding the activation and radiological emission from Tungsten is important for maintenance planning and decommissioning. Using irradiation simulations (generated using FISPACT-II (Sublet et al., 2017) and including expected impurities in the Tungsten composition) from studies (Gilbert et al., 2019, 2018) of the EU DEMO fusion reactor concept (Harman, 2012; EUROfusion, 2023) the  $\beta^-$  and  $\beta^-$ -induced Bremsstrahlung spectra have been calculated using the  $\beta$ -library. These are shown in Fig. 8 alongside the predicted  $\gamma$ -spectrum at the end of irradiation, approximating component end of life ( $\approx 5$  full power year for EU DEMO). It can be seen from the upper panel of Fig. 8 that the Bremsstrahlung contribution to the materials  $\gamma$  spectra is peaked at low energies but extends to higher energies than the traditional decay  $\gamma$ -lines, albeit at a much reduced intensity. At this time, immediately after shut-down, this inventory is dominated by short-lived  $\beta^-$ -emitting nuclides, so Bremsstrahlung has a significant contribution to total photon emission. This will diminish quickly as these nuclides are allowed to decay. The lower panel, which shows the derived  $\beta^-$

spectrum, reveals that the highest energy  $\beta^-$ -emissions arise from short lived nuclides  $^{12}\text{B}$  (half-life of 0.02 s) and  $^{16}\text{N}$  (half-life of 7.13 s). As such it can be expected that high energy tail of the  $\beta^-$  spectrum, and the Bremsstrahlung spectrum, would diminish quickly. This is confirmed by Fig. 9, which shows equivalent results after 7 days of cooling, here no  $^{12}\text{B}$  and  $^{16}\text{N}$  are present and the maximum predicted energy of the  $\beta^-$  and Bremsstrahlung spectra has reduced. Both  $^{12}\text{B}$  and  $^{16}\text{N}$  are sourced from impurities within the Tungsten definition, highlighting the need for impurity control in fusion materials. Spectra such as those shown in Figs. 8 and 9 could be found for all times of interest. From this a complete time-dependant  $\beta$ -spectra response can be derived and used to aid spectrometry studies.

## 6. Conclusion

A library of continuum  $\beta - \nu$  spectra, named BNBSL, has been developed from the code *BetaShape* and ENSDF data. This has been extended beyond *BetaShape* via the inclusion of complete Bremsstrahlung probability distributions which can be used to find the Bremsstrahlung photon spectrum on any grid spacing a user requires. This library is intended for use with inventory simulations for nuclear applications.

The library's content has been compared to available experimental data and existing decay data libraries. It has been shown that the included spectra generally have good agreement to experimental data but some do require improvement. These spectra have been included despite the apparent lower quality to guarantee coverage. The mean energies extracted from the continuum spectra show similar levels of agreement with experiment as existing decay data. This suggests that they may share a common origin, likely ENSDF data used as input. Poorer agreement with experiment may be a result of ambiguous nuclear structure information. For example, if the difference in angular momentum between initial and final states is not known an approximate Shape factor cannot be determined. Also, approximate descriptions of the nuclear matrix element for forbidden non-unique beta decays will impact the predictive power of such models. As such the resulting spectrum shape will likely be incorrect. This highlights

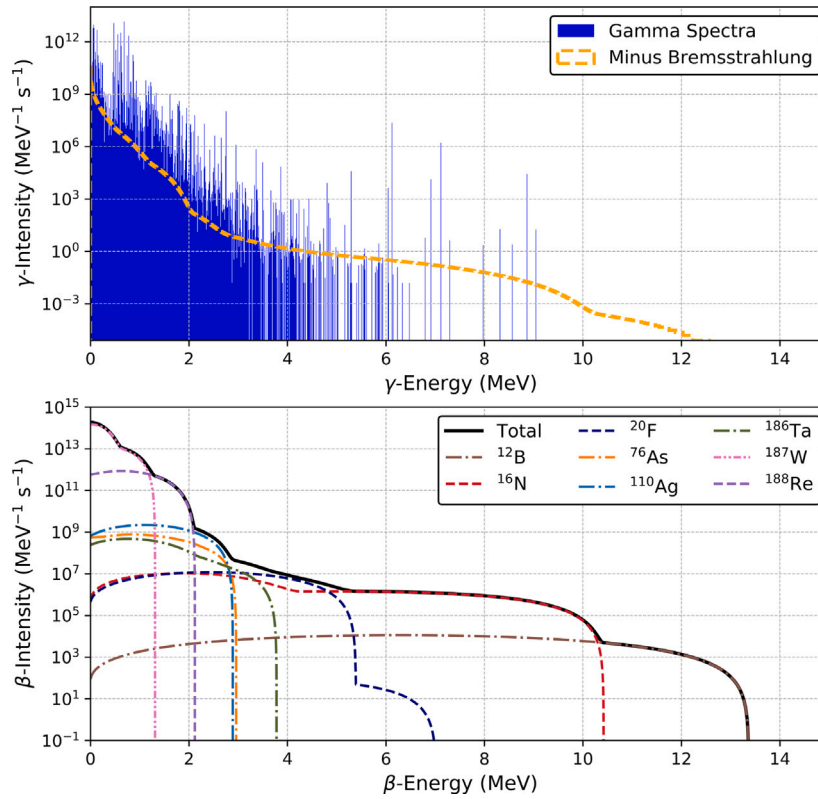


Fig. 8. Results for *first wall tungsten* in a fusion reactor at shut down found using the TENDL19 cross section library (Koning et al., 2019) and decay2020 decay data (decay2020, 2021). The upper panel shows the expected  $\gamma$ -spectrum alongside the  $\beta^-$  Bremsstrahlung contribution. The lower panel shows the  $\beta^-$ -spectrum for the material, with contributions from nuclides with provide a significant contribution to the total spectrum.  $\beta$ -energy is the kinetic energy of the  $\beta$ .

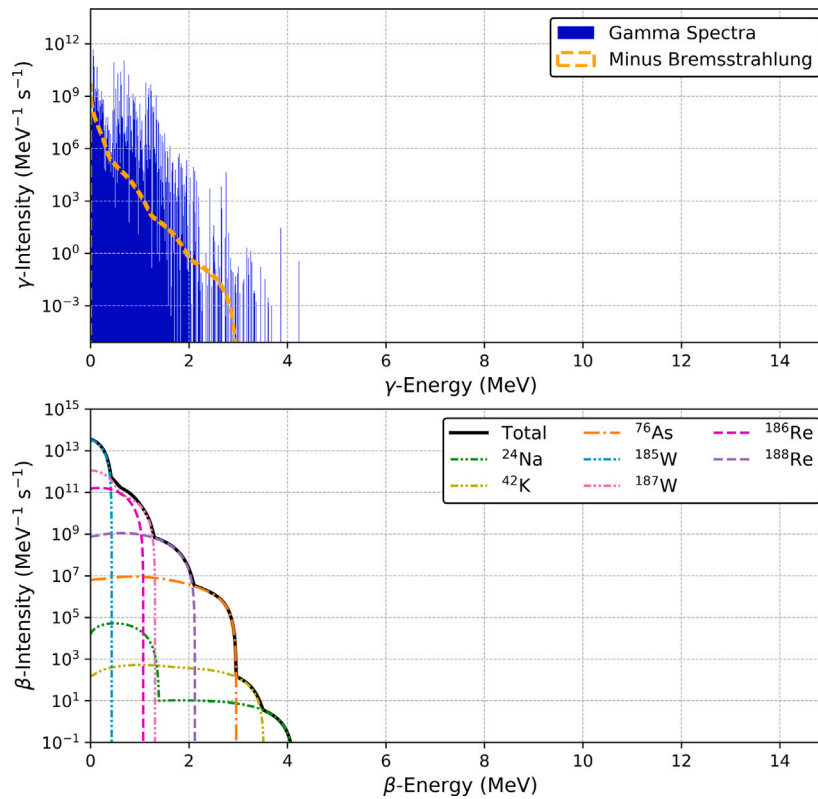


Fig. 9. Results for *first wall Tungsten* in a fusion reactor 7 days after shut down found using the TENDL19 cross section library (Koning et al., 2019) and decay2020 decay data (decay2020, 2021). The upper panel shows the expected  $\gamma$ -spectrum alongside the  $\beta^-$  Bremsstrahlung contribution. The lower panel shows the  $\beta^-$ -spectrum for the material, with contributions from nuclides with provide a significant contribution to the total spectrum.  $\beta$ -energy is the kinetic energy of the  $\beta$ , scale is identical to Fig. 8 for comparison.

a continued need for high fidelity  $\beta$ -decay measurements and nuclear structure theory such that knowledge of  $\beta$ -transitions, as well as other nuclear decays, can be improved.

The library produced in this work represents the most complete set of  $\beta$ - $\nu$  continuum spectra available at time of writing. Any application which requires detailed knowledge of  $\beta$  and/or  $\nu$  emissions should consider the results of this work as part of the analysis. It is hoped that future advancements in  $\beta$ -decay and nuclear structure theory alongside more complete experimental data will allow updated and expanded versions of this library to be produced. The functionality to evaluate the  $\beta$ - $\nu$  continuum spectra for a calculated inventory will be available in version 6 of the activation-transmutation code FISPACT-II (release forthcoming).

### CRedit authorship contribution statement

**G.W. Bailey:** Writing – review & editing, Writing – original draft, Visualization, Validation, Software, Methodology, Investigation, Formal analysis, Conceptualization. **C. Dronne:** Validation, Formal analysis. **D. Foster:** Writing – review & editing, Formal analysis. **M.R. Gilbert:** Writing – review & editing, Supervision.

### Declaration of competing interest

The authors declare that they have no known competing financial interests or personal relationships that could have appeared to influence the work reported in this paper.

### Data availability

Data will be made available on request.

### Acknowledgements

This work has been funded by the EPSRC Energy Programme, United Kingdom [grant number EP/W006839/1]. To obtain further information on the data and models underlying this paper please contact PublicationsManager@ukaea.uk. For the purpose of open access, the author(s) has applied a Creative Commons Attribution (CC BY) licence (where permitted by UKRI, 'Open Government Licence' or 'Creative Commons Attribution No-derivatives (CC BY-ND) licence' may be stated instead) to any Author Accepted Manuscript version arising.

The authors would like to thank A. Algora who made experimental data available for use in this work.

### References

- Algora, A., Tain, J.L., Rubio, B., Fallot, M., Gelletly, W., 2021. Beta-decay studies for applied and basic nuclear physics. *Eur. Phys. J. A* 57 (3), 85. <http://dx.doi.org/10.1140/epja/s10050-020-00316-4>.
- Bloch, F., 1936. On the continuous  $\gamma$ -radiation accompanying the  $\beta$ -decay. *Phys. Rev.* 50, 272–278. <http://dx.doi.org/10.1103/PhysRev.50.272>.
- Bodenstein-Dresler, L., Chu, Y., Gehre, D., Gößling, C., Heimbald, A., Herrmann, C., Hodak, R., Kostensalo, J., Kröniger, K., Küttler, J., Nitsch, C., Quante, T., Rukhadze, E., Stekl, I., Suhonen, J., Tebrügge, J., Temminghoff, R., Volkmer, J., Zatschler, S., Zuber, K., 2020. Quenching of  $g_A$  deduced from the  $\beta$ -spectrum shape of  $^{113}\text{Cd}$  measured with the COBRA experiment. *Phys. Lett. B* 800, 135092. <http://dx.doi.org/10.1016/j.physletb.2019.135092>, URL <https://www.sciencedirect.com/science/article/pii/S0370269319308147>.
- Boehm, F., Wu, C.S., 1954. Internal bremsstrahlung and ionization accompanying beta decay. *Phys. Rev.* 93, 518–523. <http://dx.doi.org/10.1103/PhysRev.93.518>.
- Brown, D., et al., 2018. ENDF/B-VIII.0: the 8th major release of the nuclear reaction data library with CIELO-project cross sections, new standards and thermal scattering data. *Nucl. Data Sheets* 148, 1–142. <http://dx.doi.org/10.1016/j.nds.2018.02.001>, Special Issue on Nuclear Reaction Data.
- Bühning, W., 1984. The screening correction to the Fermi function of nuclear  $\beta$ -decay and its model dependence. *Nuclear Phys. A* 430 (1), 1–20. [http://dx.doi.org/10.1016/0375-9474\(84\)90190-8](http://dx.doi.org/10.1016/0375-9474(84)90190-8).
- Cengiz, A., Almaz, E., 2004. Internal bremsstrahlung spectra of  $\beta$ -particle emitters using the Monte Carlo method. *Radiat. Phys. Chem.* 70 (6), 661–668. <http://dx.doi.org/10.1016/j.radphyschem.2004.03.008>.

- Chang, C.S.W., Falkoff, D.L., 1949. On the continuous Gamma-radiation accompanying the beta-decay of nuclei. *Phys. Rev.* 76, 365–371. <http://dx.doi.org/10.1103/PhysRev.76.365>.
- Curtis, M.L., 1972. Detection and measurement of tritium by bremsstrahlung counting. *Int. J. Appl. Radiat. Isot.* 23 (1), 17–23. [http://dx.doi.org/10.1016/0020-708X\(72\)90097-X](http://dx.doi.org/10.1016/0020-708X(72)90097-X).
- decay2020, 2021. URL [https://fispact.ukaea.uk/nuclear\\_data/decay2020.tar.bz2](https://fispact.ukaea.uk/nuclear_data/decay2020.tar.bz2).
- Dillman, L., 1980. EDISTR: A Computer Program to Obtain a Nuclear Decay Data Base for Radiation Dosimetry. ORNL/TM-6689, United States.
- Eckerman, K.F., Westfall, R.J., Ryman, J.C., Cristy, M., 1994. Availability of nuclear decay data in electronic form, including beta spectra not previously published. *Health Phys.* 67, 338–345. <http://dx.doi.org/10.1097/00004032-199410000-00004>.
- EUROfusion, 2023. The demonstration power plant: DEMO. Available at <https://eurofusion.org/programme/demo/> (16/3/2023).
- Ghorbani, M., Hashempour, M., Amato, E., Knaup, C., 2019. Effect of beta particles spectrum on absorbed fraction in internal radiotherapy. *Asia Ocean. J. Nucl. Med. Biol.* 7 (1), 71–83. <http://dx.doi.org/10.22038/aojnmb.2018.11610>.
- Gilbert, M.R., Eade, T., Bachmann, C., Fischer, U., Taylor, N.P., 2018. Waste assessment of European DEMO fusion reactor designs. *Fus. Eng. Des.* 136, 42–48. <http://dx.doi.org/10.1016/j.fusengdes.2017.12.019>, Special Issue: Proceedings of the 13th International Symposium on Fusion Nuclear Technology (ISFNT-13).
- Gilbert, M.R., Eade, T., Rey, T., Vale, R., Bachmann, C., Fischer, U., Taylor, N.P., 2019. Waste implications from minor impurities in European DEMO materials. *Nucl. Fus.* 59, 076015. <http://dx.doi.org/10.1088/1741-4326/ab154e>.
- Group, C.S.E.W., 2018. ENDF-6 Formats Manual. Tech. Rep. BNL-203218-2018-INRE, Brookhaven National Laboratory.
- Harman, J., 2012. DEMO Operational Concept Description. Tech. Rep. report number: 2LCY7A, EUROfusion/EFDA.
- Hayen, L., Kostensalo, J., Severijns, N., Suhonen, J., 2019a. First-forbidden transitions in reactor antineutrino spectra. *Phys. Rev. C* 99, 031301. <http://dx.doi.org/10.1103/PhysRevC.99.031301>, URL <https://link.aps.org/doi/10.1103/PhysRevC.99.031301>.
- Hayen, L., Kostensalo, J., Severijns, N., Suhonen, J., 2019b. First-forbidden transitions in the reactor anomaly. *Phys. Rev. C* 100, 054323. <http://dx.doi.org/10.1103/PhysRevC.100.054323>, URL <https://link.aps.org/doi/10.1103/PhysRevC.100.054323>.
- Hayen, L., Severijns, N., 2019. Beta spectrum generator: High precision allowed  $\beta$  spectrum shapes. *Comput. Phys. Comm.* 240, 152–164. <http://dx.doi.org/10.1016/j.cpc.2019.02.012>.
- Huber, P., 2016. Reactor antineutrino fluxes – status and challenges. *Nuclear Phys. B* 908, 268–278. <http://dx.doi.org/10.1016/j.nuclphysb.2016.04.012>, Neutrino Oscillations: Celebrating the Nobel Prize in Physics 2015.
- ICRP, 2008. Nuclear Decay Data for Dosimetric Calculations, Vol. 107. Tech. Rep. Ann.ICRP 38(3), ICRP Publication.
- Iwamoto, O., Iwamoto, N., Shibata, K., Ichihara, A., Kunieda, S., Minato, F., Nakayama, S., 2020. Status of JENDL. EPJ Web Conf. 239, 09002. <http://dx.doi.org/10.1051/epjconf/202023909002>.
- Knipp, J.K., Uhlenbeck, G.E., 1936. Emission of gamma radiation during the beta decay of nuclei. *Physica* 3 (6), 425–439. [http://dx.doi.org/10.1016/S0031-8914\(36\)80008-1](http://dx.doi.org/10.1016/S0031-8914(36)80008-1).
- Koning, A., Rochman, D., Sublet, J.-C., Dzysiuik, N., Fleming, M., van der Marck, S., 2019. TENDL: Complete nuclear data library for innovative nuclear science and technology. *Nucl. Data Sheets* 155, 1–55. <http://dx.doi.org/10.1016/j.nds.2019.01.002>, Special Issue on Nuclear Reaction Data.
- Leder, A.F., Mayer, D., Ouellet, J.L., Danevich, F.A., Dumoulin, L., Giuliani, A., Kostensalo, J., Kotila, J., de Marcillac, P., Nones, C., Novati, V., Olivieri, E., Poda, D., Suhonen, J., Tretyak, V.I., Winslow, L., Zolotarova, A., 2022. Determining  $g_A/g_V$  with high-resolution spectral measurements using a  $\text{LiInSe}_2$  bolometer. *Phys. Rev. Lett.* 129, 232502. <http://dx.doi.org/10.1103/PhysRevLett.129.232502>, URL <https://link.aps.org/doi/10.1103/PhysRevLett.129.232502>.
- Matsuyama, M., Torikai, Y., Watanabe, K., 2005. In-situ measurement of high level tritiated water by bremsstrahlung counting. *Fusion Sci. Technol.* 48 (1), 324–331. <http://dx.doi.org/10.13182/FST48-324>.
- Mougeot, X., 2015a. Erratum: Reliability of usual assumptions in the calculation of  $\beta$  and  $\nu$  spectra [phys. Rev. C 91, 055504 (2015)]. *Phys. Rev. C* 92, <http://dx.doi.org/10.1103/PhysRevC.92.059902>.
- Mougeot, X., 2015b. Reliability of usual assumptions in the calculation of  $\beta$  and  $\nu$  spectra. *Phys. Rev. C* 91, 055504. <http://dx.doi.org/10.1103/PhysRevC.91.055504>.
- Mougeot, X., 2015c. Reliability of usual assumptions in the calculation of  $\beta$  and  $\nu$  spectra. *Phys. Rev. C* 91, <http://dx.doi.org/10.1103/PhysRevC.91.055504>.
- Mougeot, X., 2015d. Systematic comparison of beta spectra calculations using improved analytical screening correction with experimental shape factors. *Appl. Radiat. Isot.* 109, <http://dx.doi.org/10.1016/j.apradiso.2015.11.030>.
- Mougeot, X., 2017. BetaShape: A new code for improved analytical calculations of beta spectra. EPJ Web Conf. 146, 12015. <http://dx.doi.org/10.1051/epjconf/201714612015>.
- NNDC, 2019. URL <https://www.nndc.bnl.gov/ensdf/>.
- Plompen, A.J.M., et al., 2020. The joint evaluated fission and fusion nuclear data library, JEFF-3.3. *Eur. Phys. J. A* 56 (7), 181.
- RADAR decay data, 2019. URL <https://www.doseinfo-radar.com/RADARdecay.html>.

- Rudstam, G., Johansson, P.-I., Tengblad, O., Aagaard, P., Eriksen, J., 1990. Beta and gamma spectra of short-lived fission products. *At. Data Nucl. Data Tables* 45, 239–320. [http://dx.doi.org/10.1016/0092-640X\(90\)90009-9](http://dx.doi.org/10.1016/0092-640X(90)90009-9).
- Shu, W., Matsuyama, M., Suzuki, T., Nishi, M., 2004. Characteristics of a promising tritium process monitor detecting bremsstrahlung X-rays. *Nucl. Instrum. Methods Phys. Res. A* 521 (2), 423–429. <http://dx.doi.org/10.1016/j.nima.2003.10.110>.
- Sirlin, A., 1967. General properties of the electromagnetic corrections to the beta decay of a physical nucleon. *Phys. Rev.* 164, 1767–1775. <http://dx.doi.org/10.1103/PhysRev.164.1767>.
- Sirlin, A., 2011. Radiative correction to the  $\bar{\nu}_e(\nu_e)$  spectrum in  $\beta$  decay. *Phys. Rev. D* 84, 014021. <http://dx.doi.org/10.1103/PhysRevD.84.014021>.
- Stabin, M.G., da Luz, L.C., 2002. Decay data for internal and external dose assessment. *Health Phys.* 83, 471–475. <http://dx.doi.org/10.1097/00004032-200210000-00004>.
- Sublet, J.C., Eastwood, J.W., Morgan, J.G., Gilbert, M.R., Fleming, M., Arter, W., 2017. FISPACT-II: An advanced simulation system for activation, transmutation and material modelling. *Nucl. Data Sheets* 139, 77–137. <http://dx.doi.org/10.1016/j.nds.2017.01.002>.
- UKAEA, 2023. FISPACT-II Nuclear data. Available at <https://fispact.ukaea.uk/nuclear-data/downloads/> (16/3/2023).
- Valencia, E., et al., 2017. Total absorption  $\gamma$ -ray spectroscopy of the  $\beta$ -delayed neutron emitters  $^{87}\text{Br}$ ,  $^{88}\text{Br}$ , and  $^{94}\text{Rb}$ . *Phys. Rev. C* 95, 024320. <http://dx.doi.org/10.1103/PhysRevC.95.024320>.